JACS
JOURNAL OF THE AMERICAN CHEMICAL SOCIETY

ARTICLE

pubs.acs.org/JACS

Highly Polar Carbohydrates Stack onto DNA Duplexes via CH/π Interactions

Ricardo Lucas,[†] Irene Gómez-Pinto,[‡] Anna Aviñó,[§] Jose J. Reina,[†] Ramón Eritja,[§] Carlos González,[‡] and Juan C. Morales*[,†]

[†]Department of Bioorganic Chemistry, Instituto de Investigaciones Químicas, CSIC − Universidad de Sevilla, Americo Vespucio, 49, 41092 Sevilla, Spain

[‡]Instituto de Química Física "Rocasolano", CSIC, C/Serrano 119, 28006 Madrid, Spain

[§]Instituto de Investigación Biomédica de Barcelona, IQAC, CSIC, CIBER − BBN Networking Centre on Bioengineering, Biomaterials and Nanomedicine, Baldiri Reixac 10, E-08028 Barcelona, Spain

Supporting Information

ABSTRACT: Carbohydrate−nucleic acid contacts are known to be a fundamental part of some drug−DNA recognition processes. Most of these interactions occur through the minor groove of DNA, such as in the calicheamicin or anthracycline families, or through both minor and major groove binders such as in the pluramycins. Here, we demonstrate that carbohydrate−DNA interactions are also possible through sugar capping of a DNA double helix. Highly polar mono- and disaccharides are capable of CH/π stacking onto the terminal DNA base pair of a duplex as shown by NMR spectroscopy. The energetics of the carbohydrate−DNA interactions vary depending on the stereochemistry, polarity, and contact surface of the sugar involved and also on the terminal base pair. These results reveal carbohydrate−DNA base stacking as a potential recognition motif to be used in drug design, supramolecular chemistry, or biobased nanomaterials.

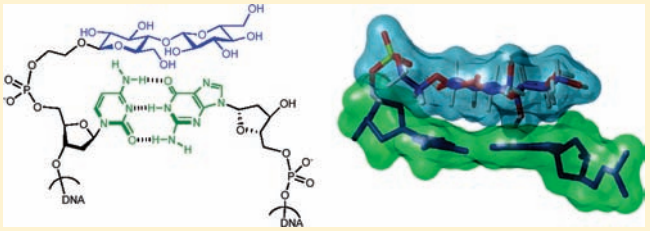

INTRODUCTION

Molecular interactions between biomolecules are crucial for a huge number of biological processes. Hydrogen bonding and electrostatic interactions are among the best understood noncovalent forces that participate in this biomolecular recognition. In contrast, aromatic stacking, CH/π, or hydrophobic interactions are quite less understood. Factors contributing to aromatic $\pi-\pi$ stacking have been examined using small organic structures, such as in the early studies by the groups of Rebek,[1] Gellman,[2] and Dougherty.[3] An alternative approach employed the "dangling-end" effect in DNA and RNA duplexes, which occurs when a single unpaired base is added at the end of a duplex. In this context, natural[4] and non-natural hydrophobic nucleobases[5] stabilize the duplexes by stacking interactions. Likewise, other aromatics such as quinolones,[6] stilbenes,[7] polycyclic aromatic hydrocarbons,[8] or porphyrins[9] linked through a variety of spacers to the 3′- or 5′-end of oligonucleotide strands have also shown enhanced stabilization of DNA duplexes. In addition, nonpolar nucleobases, such as pyrene[10] or biphenyl nucleosides,[11] have proven to be efficient in stabilizing DNA by interstrand aromatic stacking interactions. Nevertheless, planar aromaticity is not a requisite for stacking interactions in the environment of DNA. Leumann et al. have shown that a nonaromatic hydrophobic residue, a phenylcyclohexyl nucleoside, can be sandwiched inside DNA and contribute favorably to duplex stability.[12] Similarly, steroid derivatives, such as cholic acid, demonstrated to stabilize duplexes through CH/π stacking when placed as a dangling-end motif.[13] Recently, carbohydrate−phenyl stacking interactions using a dangling-end DNA duplex model system have been also quantified.[14] The energetic contributions of this interaction range from −0.15 to −0.40 kcal mol^{-1} and depend on the number of hydroxyl groups, the stereochemistry, and the presence of a methyl group in the sugar moiety.

The aim of this work is to explore carbohydrate−DNA interactions making use of the dangling-end DNA model. Our model system consists of carbohydrate−DNA conjugates where different mono- and dissacharides are attached to the 5′-end of DNA strands (Figure 1a). Carbohydrate−DNA contacts have been reported in different drug−DNA recognition processes, mostly through the minor groove, such as in DNA intercalant anthracyclines[15] or in the calicheamicin family,[16] and through both minor and major groove, such as in the pluramycins.[17] Sugar−oligonucleotide stacking interactions have only been described in antibiotic-RNA recognition,[18] where the 2′-amino-2′-deoxyglucose moiety of different aminoglycosides stacks over guanine 1491 of the 16S rRNA A-site. This specific interaction has never been studied or quantified. Herein, we report on the synthesis, stability, sequence-selectivity, and structural features of mono- and disaccharide oligonucleotide conjugates where the highly polar sugar moieties have

Received: October 5, 2010
Published: January 18, 2011

dx.doi.org/10.1021/ja108962j | J. Am. Chem. Soc. 2011, 133, 1909–1916

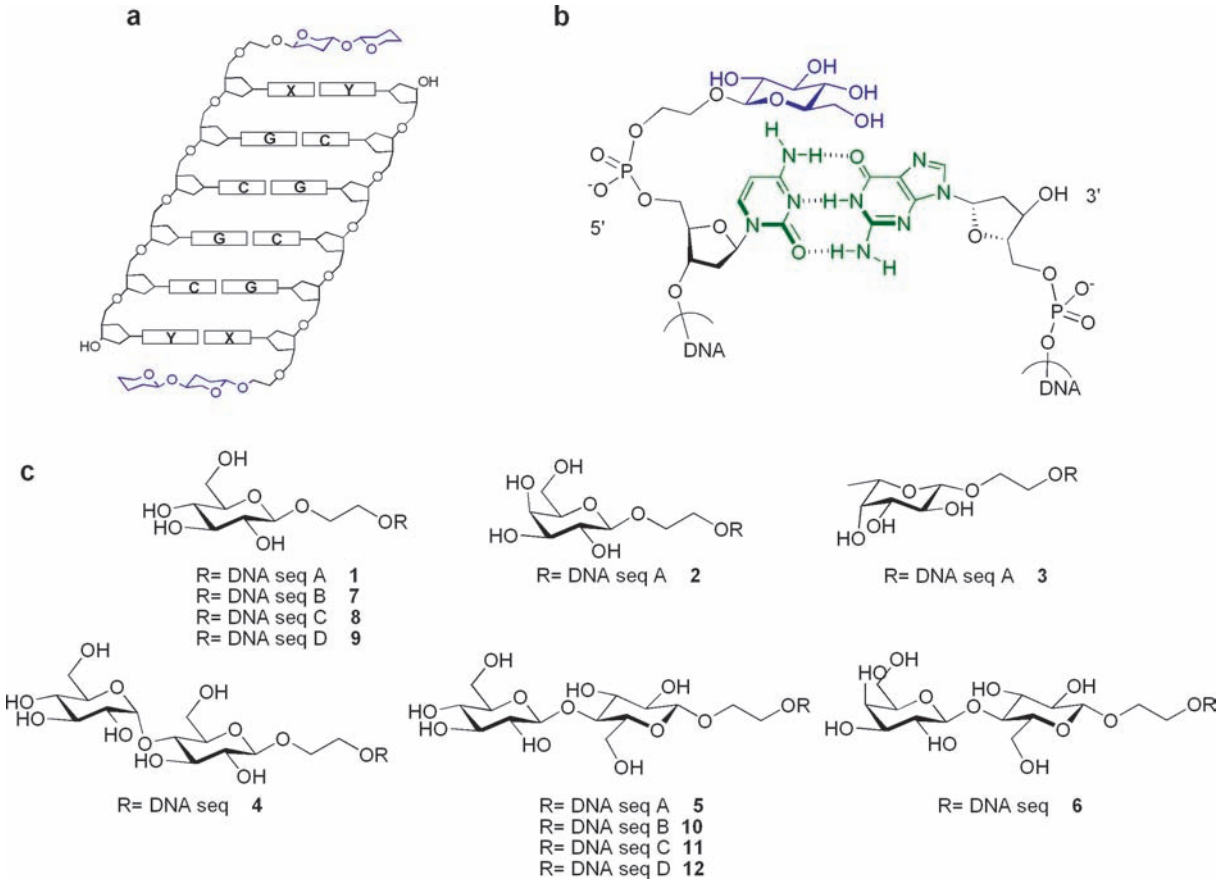

Figure 1. Description of the oligonucleotide conjugate under study. (a) Schematic drawing of the dangling-ended DNA designed to study carbohydrate−DNA interactions. (b) Enlarged view of the dangling-end area of a monosaccharide−oligonucleotide conjugate. (c) Carbohydrate−oligonucleotide conjugates included in the study. DNA seq A = OPO_2^-−CGCGCG, DNA seq B = OPO_2^-−GGCGCC, DNA seq C = OPO_2^-−TGCGCA, DNA seq D = OPO_2^-−AGCGCT. Control DNA sequences are CGCGCG **13**, GGCGCC **14**, TGCGCA **15**, AGCGCT **16**.

shown to stack onto DNA duplexes and stabilize sequences with terminal C−G or G−C base pairs.

RESULTS AND DISCUSSION

Design and Synthesis of the Carbohydrate−Oligonucleotide Conjugates. Inspiration for the design of the sugar−DNA conjugates (**1**−**12**) comes from previous studies on aromatic stacking where different organic platforms have been attached to the 5′-end of a short oligonucleotide.[5a,19] A short ethylene glycol spacer was selected to link the sugar moiety to the final phosphate group of the DNA strand. This length of the linker allows the location of the pyranose ring on top of the base pair to the same distance found in a nucleoside between the base and its corresponding phosphate group (Figure 1b). It is important to underline that the selected spacer is quite flexible, allowing the carbohydrate either to contact the DNA base pair or to be immersed in bulk water. Preparation of the saccharide−oligonucleotide conjugates was performed by standard solid-phase oligonucleotide automatic synthesis using the corresponding carbohydrate phosphoramidites. Three monosaccharides, β-D-glucose, β-D-galactose, and β-L-fucose (Figure 1c), were selected to compare the influence of the stereochemistry and polarity in the interaction with the DNA duplexes. Disaccharide oligonucleotide conjugates were prepared to study the influence in the interaction of the surface enlargement of the carbohydrate moiety, the increase in the number of hydroxyl groups, and the consequent increase in polarity. 1→4-Linked disaccharides, β-D-maltose, β-D-cellobiose, and β-D-lactose (Figure 1c), were selected due to their relative rigidity because only one oxygen atom connects the pyranose rings and also to compare the stereochemistry at the pyranose ring and at the interglycosidic position.

The synthesis of the disaccharide phosphoramidites **17**−**19** (see Figure 2) was carried out following the same methodology described previously for the monosaccharide phosphoramidites.[14] Briefly, classical glycosylation chemistry from the peracetylated bromo disaccharides was performed to attach the ethylene glycol spacer followed by standard phosphoramidite preparation.

Energetics of Carbohydrate−DNA Interactions. The influence of a 5′-sugar cap on the stability of a self-complementary short DNA sequence was measured by UV-monitored thermal denaturation experiments in a pH 7.0 phosphate buffer containing 1 M NaCl. Thermodynamic parameters were calculated from the average values obtained from melting curve fitting and linear plots of $1/T_m$ versus ln[conjugate].[4a,20] All the conjugates appear to behave in a two-state fashion, indicating cooperative interactions by the dangling residues (see melting curve examples in Figure S1 and van't Hoff plots in Figure S2). Thermodynamic parameters for the carbohydrate−oligonucleotide conjugates **1**−**6** are shown in Table 1. All mono- and disaccharides stabilize the duplex relative to the core sequence CGCGCG, with the disaccharides showing, in general, more stabilization than the monosaccharide moieties. Stabilization by the monosaccharides ranges from −0.4 to −0.6 kcal mol^{-1}, and *T*m

dx.doi.org/10.1021/ja108962j |*J. Am. Chem. Soc.* 2011, 133, 1909–1916

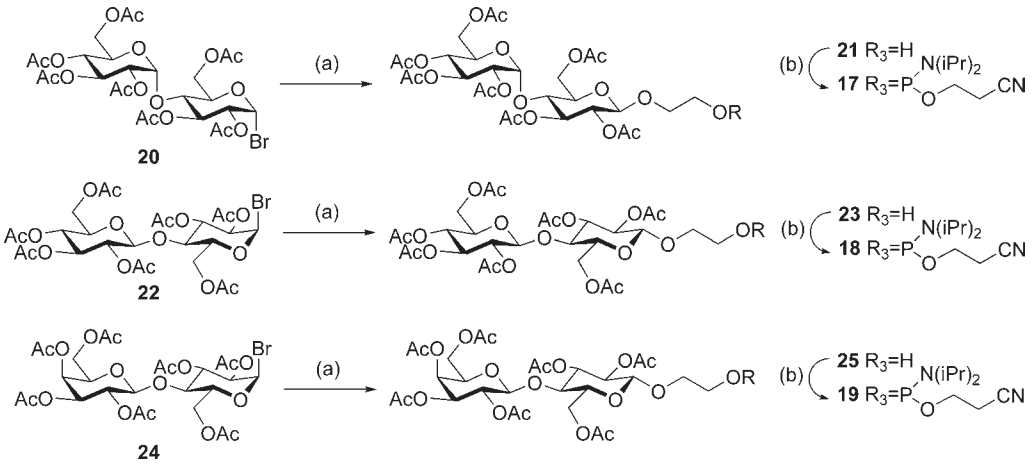

Figure 2. Synthetic route for the preparation of disaccharide phophoramidites **17**−**19**. (a) ethylene glycol, Ag_2CO_3, CH_2Cl_2, r.t., 24 h, 49−56%; (b) 2-cyanoethyl-*N*,*N*′-diisopropylamino-chlorophosphoramidite, DIEA, CH_2Cl_2, r.t., 2 h, 85−93%.

Table 1. Thermodynamic Parameters for Carbohydrate Oligonucleotide Conjugate Duplexes Containing the CGCGCG Sequence

dangling moiety[a,b,c,d]		T_m (°C)[e]	$-\Delta H°$ (kcal/mol)	$-\Delta S°$ (cal/K·mol)	$-\Delta G_{37}°$ (kcal/mol)	$\Delta\Delta G_{37}°$ (kcal/mol)
(none)	**13**	40.9	46.5	123	8.2	
glucose−C2	**1**	44.0	52.1	140	8.7	−0.5
galactose−C2	**2**	44.4	47.4	125	8.6	−0.4
fucose−C2	**3**	44.4	51.1	136	8.8	−0.6
maltose−C2	**4**	45.8	53.5	143	9.0	−0.8
cellobiose−C2	**5**	45.9	49.2	130	8.9	−0.7
lactose−C2	**6**	45.6	45.9	120	8.8	−0.6
cytosine[f]		46.2	50.4	133	9.0	−0.8
thymidine[f]		48.1	47.9	125	9.2	−1.0
benzene[f,g]		48.3	51.4	135	9.4	−1.2

[a] Core sequence is CGCGCG. [b] −C2− states for $-CH_2-CH_2-OPO_2^-$−. [c] Buffer: 10 mM Na·phosphate, 1 M NaCl, pH 7.0. [d] Estimated errors are: $T_m \pm 0.9$ °C and ±6% in $\Delta G°$. [e] Average value of three experiments measured at 5 μM conc. [f] Data from ref 5b. [g] Benzene corresponds to benzene nucleoside.

values get increased 3.1 to 3.5 °C, revealing small differences depending on the stereochemistry and the polarity of the sugar. Fucose is the most stabilizing among the monosaccharide studied, increasing the T_m of the conjugate by 3.5 °C and contributing −0.6 kcal mol^{-1} to DNA stability, −0.30 for each sugar/cytosine pair. In the case of the disaccharide units, the stabilization of the DNA conjugate increased up to −0.8 kcalmol^{-1} and T_m values raised by 4.7−5.0 °C. Again, small differences are observed among the disaccharides, with maltose being the most stabilizing and lactose the least one. In the case that both pyranose units in each disaccharide stack on top of the C−G base pair, one could expect that the stabilization would be at least double that of a single monosaccharide−single base pair (−0.8 to −1.2 kcal mol^{-1}), but this is not the case. In fact, the stabilization of the DNA duplex is slightly lower than those values most probably due to the entropic cost of freezing the two torsional angles of the interglycosidic bond. Nevertheless, it is quite remarkable that these highly polar carbohydrates, the log *P* values of which range from −1.16 to −3.76, display stability in this DNA context similar to that of planar aromatic nucleosides, such as thymidine, cytosine, or a benzene nucleoside,[5b] the log *P* values of which are −0.47, −0.36, and 2.52, respectively (Table 2). It is important to consider that the carbohydrates are linked to the DNA strand through an ethylene glycol linker, which is much more flexible than

Table 2. Molecular Weight and Partition Coefficient Data for Dangling Moieties Studied[a]

dangling moiety	MW	calc. log *P*
methyl glucoside	194.2	−2.01
methyl galactoside	194.2	−2.01
methyl fucoside	178.2	−1.16
methyl maltoside	356.3	−3.76
methyl lactoside	356.3	−3.76
methyl cellobioside	356.3	−3.76
methyl cytosine	125.1	−0.47
methyl thymine	140.1	−0.36
toluene	92.1	2.52
cholesterol	386.6	7.39
dihydroxycholesterol	418.6	5.27

[a] The log *P* values were calculated using Crippen's fragmentation[41] in the ChemBioDraw Ultra 11.0 software.

Table 3. Thermodynamic Parameters for Carbohydrate Oligonucleotide Conjugate Duplexes in Different DNA Sequence Context

X-DNA sequence[a,b,c]		T_m (°C)[d]	$-\Delta H°$ (kcal/mol)	$-\Delta S°$ (cal/K·mol)	$-\Delta G_{37}°$ (kcal/mol)	$\Delta\Delta G_{37}°$ (kcal/mol)
X = none						
CGCGCG	**13**	40.9	46.5	123	8.2	
GGCGCC	**14**	37.6	45.6	122	7.8	
TGCGCA	**15**	34.8	37.8	99	7.2	
AGCGCT	**16**	33.5	40.3	107	7.1	
X = glucose−C2						
CGCGCG	**1**	44.0	52.1	140	8.7	−0.5
GGCGCC	**7**	42.2	46.7	124	8.3	−0.5
TGCGCA	**8**	34.2	47.8	131	7.2	0.0
AGCGCT	**9**	33.6	37.3	98	7.0	0.1
X = cellobiose−C2						
CGCGCG	**5**	45.9	49.2	130	8.9	−0.7
GGCGCC	**10**	44.2	51.9	139	8.7	−0.9
TGCGCA	**11**	35.2	43.9	118	7.2	0.0
AGCGCT	**12**	34.4	39.1	103	7.1	0.0

[a] −C2− states for $-CH_2-CH_2-OPO_2^-$−. [b] Buffer: 10 mM Na·phosphate, 1 M NaCl, pH 7.0. [c] Estimated errors are: $T_m \pm 0.8$ °C and ±6% in $\Delta G°$. [d] Average value of three experiments measured at 5 μM conc.

dx.doi.org/10.1021/ja108962j |*J. Am. Chem. Soc.* 2011, 133, 1909–1916

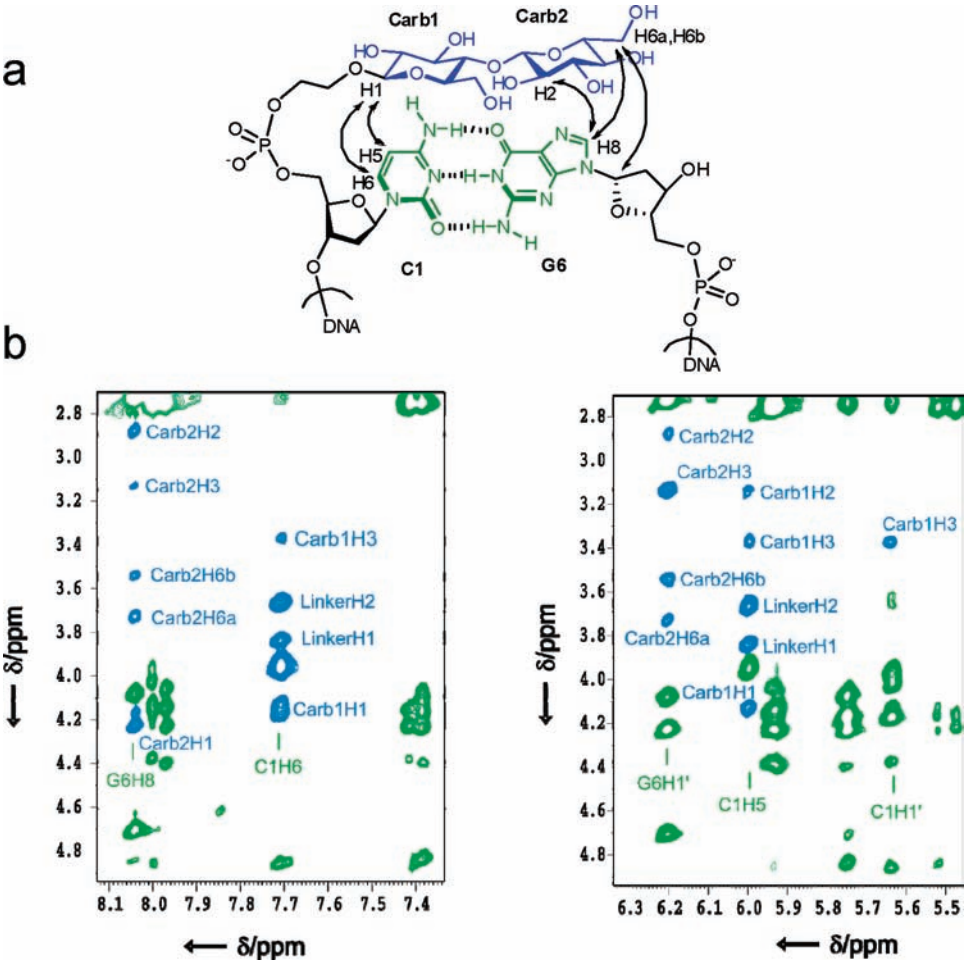

Figure 3. NOE contacts observed between sugar and DNA for cellobiose oligonucleotide conjugate **5**. (a) Schematic drawing of the conjugate where arrows correspond to the most important observed NOEs. (b) Selected regions of NOESY spectra for conjugate **5** in H_2O showing carbohydrate contacts with exchangeable and nonexchangeable protons of the terminal base-pairs. The labels represent the carbohydrates with carb1 and carb2 and the corresponding proton numbers, whereas the bases have the classical numbering scheme for DNA bases.

the deoxyribose unit of the cytosine, thymidine, or benzene nucleosides. Moreover, the only previous example of a nonplanar 5′-capping DNA compound capable of stabilizing the duplex is the very apolar cholic acid family, with log *P* values from 5.27 for cholic acid to 7.39 for cholesterol (Table 3).[13]

Sequence-Selectivity of Carbohydrate−DNA Stacking Interactions. Monosaccharide glucose and disaccharide cellobiose were selected to study sequence-selectivity on carbohydrate−DNA stacking. Terminal base pairs were varied within self-cDNA sequences (see Table 3). When a C−G or G−C base pair is at the edge of the DNA duplex (conjugates **1**, **5**, **7**, and **10**), the T_m values increased by 3−5 °C in comparison to the control sequences without sugar modification and contributed −0.5 to −0.9 kcal mol^{-1} to stability with two symmetrical substitutions. When an A−T or T−A base pair is at the edge of the duplex (conjugates **8**, **9**, **11**, and **12**), the T_m and ΔG values are very similar for the saccharide oligonucleotide conjugates and the control DNA sequences, and no additional energetic stabilization is observed. This sequence-selectivity observed for sugar preferentially stabilizing DNA duplexes with C−G or G−C base pairs is not unusual.

Santalucia et al.[21] showed that a single nucleotide dangling-end could lead to large energetic differences depending on the closing base pair type and orientation. Nevertheless, no general rules have been observed neither in the DNA nor in the RNA context. In the case of carbohydrates stacking onto DNA, more studies would be needed to shed light on the selectivity found.

Structural Features of the Carbohydrate−Oligonucleotide Conjugates. The structures of six conjugates containing either a monosaccharide or a disaccharide attached to the CGCGCG core sequence (**1**−**6**) and two conjugates containing glucose and cellobiose attached to the TGCGCA core sequence (**9** and **12**, respectively) were studied by NMR spectroscopy. Exchangeable and nonexchangeable protons of the DNA moieties were assigned following standard techniques (Table S1). Resonance of the carbohydrate moieties and the linkers were also completely assigned with a few exceptions indicated in Table S1. A comparison between the DNA chemical shifts in the conjugates and the control duplex indicates that the overall duplex structure is not distorted by the presence of the carbohydrate. Significant chemical shift changes are only observed for some protons of the terminal residues. In the case of the monosaccharide conjugates **1**−**3** and **8** (see Figure S3), this effect is limited to the 5′-terminal residue, which is directly linked to the carbohydrate. Up to 0.22 ppm downfield chemical shift is observed for H2′ of C1 in the fucose oligonucleotide conjugate **3**. In the case of the disaccharides **4**−**6** and **10** (see Figure S4), the chemical shift perturbations also affect the 3′-terminal residues of the complementary strand (G6 in conjugates **4**, **5**, and **6**, and A6 in

dx.doi.org/10.1021/ja108962j |*J. Am. Chem. Soc.* 2011, 133, 1909–1916

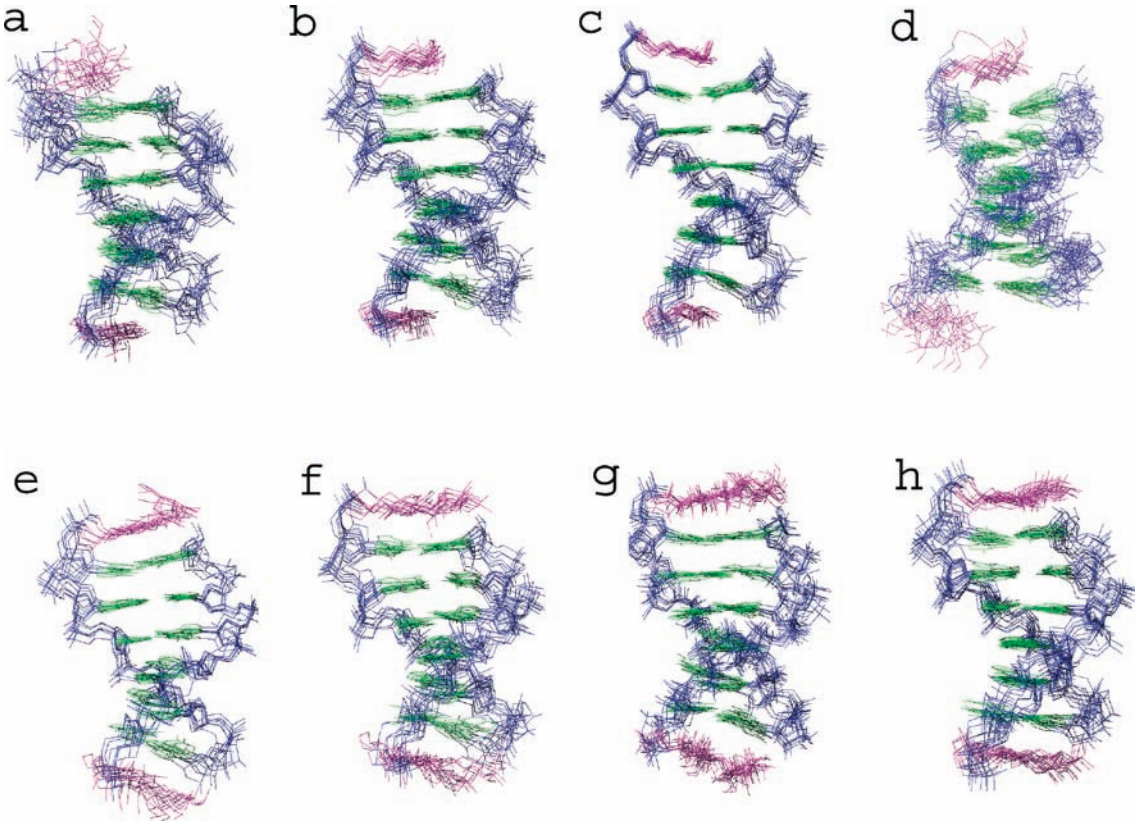

Figure 4. Ensemble of the superposition of the 10 refined structures of the monosaccharide−DNA conjugates. (a) β-D-Glucose-C2-CGCGCG conjugate **1**. (b) β-D-Galactose-C2-CGCGCG conjugate **2**. (c) β-L-Fucose-C2-CGCGCG conjugate **3**. (d) β-D-Glucose-C2-TGCGCA conjugate **8**. (e) β-D-Maltose-C2-CGCGCG conjugate **4**. (f) β-D-Cellobiose-C2-CGCGCG conjugate **5**. (g) β-D-Lactose-C2-CGCGCG conjugate **6**. (h) β-D-Cellobiose-C2-TGCGCA conjugate **11**. C2 stands for $-CH_2-OPO_2^-$−. The backbone of the oligonucleotide strands is shown in blue color, the DNA bases are in green, and the saccharides and the spacer are in purple. The figures have been prepared with MOLMOL.[40]

conjugate **12**). For example, H2′ of G6 shows a downfield chemical shift of 0.07 ppm in cellobiose oligonucleotide conjugate **5**. Most of the reported solution DNA structures contained one or two nucleotides[4b] or an aromatic moiety[22,23] as the dangling-end unit. In these cases, quite relevant chemical shifts were observed in the exchangeable and nonexchangeable protons of the terminal base pair most probably due to the presence of the ring current effect of the aromatic ring. The cholic acid−DNA conjugates, the only reported oligonucleotides with a nonaromatic dangling-end, did not report chemical shift differences for the terminal base pairs.[13]

Analysis of the NOE data indicates that the structure of the DNA is mainly a B-form double helix without significant distortions (Table S2). Interestingly, a large number of NOE contacts between the linker and the carbohydrates with the DNA are observed. The NOE contacts between the monosaccharides and the DNA are in general weak and mainly occur with the 5′-terminal residue (C1). In the case of the disaccharides (Figure 3), stronger NOE cross-peaks are observed with the 5′- and 3′-terminal residues of the complementary strand. In the four disaccharide−DNA conjugates studied, around 25 carbohydrate−DNA NOE contacts were observed (see Table S3). Of particular significance are the contacts with exchangeable protons of the terminal base-pair. These protons are not observed in the control duplex; however, they exhibit narrow signals in the disaccharide conjugates, and NOEs can be observed with other DNA and carbohydrate protons. Terminal exchangeable protons are usually not observed or present very broad signals in short DNA duplex because terminal base pairs tend to be more dynamical, and, consequently, their imino and amino protons have enhanced water exchange rates. The narrow signals observed in exchangeable protons of the terminal base-pairs in these conjugates indicate that the carbohydrates reduce the dynamics of the terminal base pairs and protect them from water exchange. Although much less pronounced, this effect is also observed in some of the monosaccharide studied here, and it has been reported in some aromatic-capped oligonucleotides.[22]

On the basis of the NMR experimental information, the structures of the carbohydrate−DNA conjugates were calculated with the AMBER package. The resulting structures are shown in Figure 4. At a first glance, the carbohydrate conformations are usual $^4C_1$ chairs for all the conjugates studied. At the same time, it can be observed that all the saccharide moieties are stacked on top of the DNA base or DNA base pair right below them. This stacking structure is possible due to CH/π interactions between carbohydrate protons of either the α or the β faces of the pyranose units and the π electron cloud of the aromatic DNA bases. This type of interactions is not frequent in oligonucleotide binding, but it is quite common in carbohydrate−protein recognition where the aromatic rings are the three aromatic amino acids Phe, Tyr, or Trp.[24] In the case of the monosaccharide conjugates, the carbohydrate interacts with its neighboring base (cytosine for conjugates **1**−**3** and thymine for **8**). Only in the case of the fucose conjugate **3** is the carbohydrate conformation

dx.doi.org/10.1021/ja108962j |J. Am. Chem. Soc. 2011, 133, 1909–1916

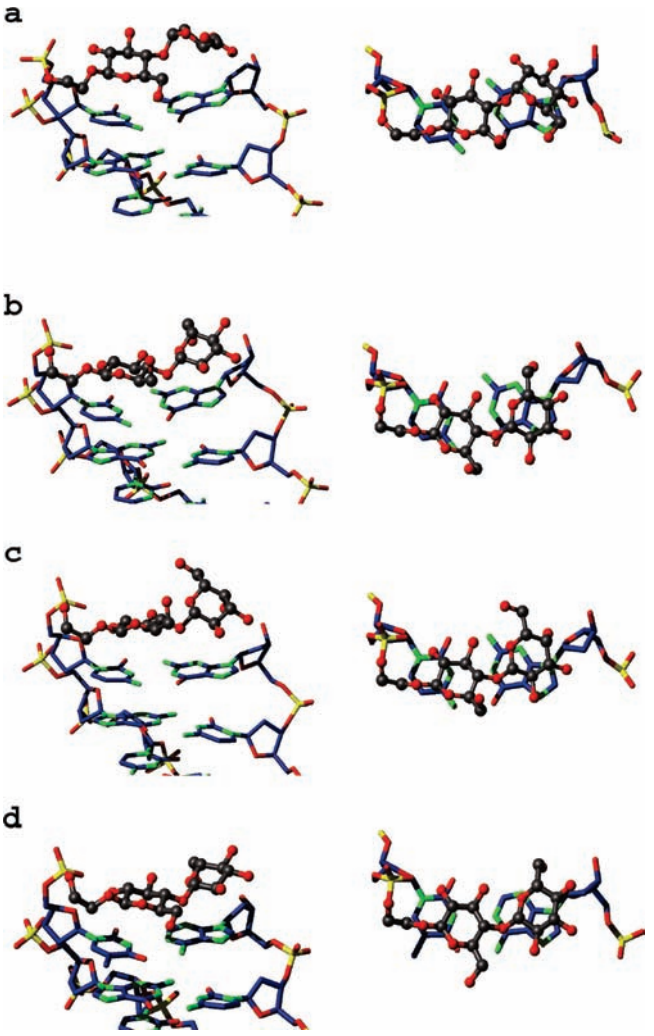

Figure 5. Details of the structures of the four disaccharide oligonucleotide conjugates. (a) β-D-Maltose-C2-CGCGCG conjugate **4**. (b) β-D-Cellobiose-C2-CGCGCG conjugate **5**. (c) β-D-Lactose-C2-CGCGCG conjugate **6**. (d) β-D-Cellobiose-C2-TGCGCA conjugate **11**. Left: Side view of the disaccharide−DNA recognition motif of each conjugate. Right: Top view of the disaccharide−DNA recognition motif of each conjugate. The figures have been prepared with MOLMOL.[40]

well-defined; stacking on top of the terminal base pair seems to be preferential through its α face. In the other monosaccharide oligonucleotide conjugates, the interaction with the terminal base occurs most probably through both faces of the carbohydrate, and the weak NOEs observed are a consequence of these multiple modes of interaction. Nevertheless, in all the disaccharide oligonucleotide conjugates, the structures are well-defined. As shown in Figure 5, the pyranose ring attached to the linker interacts with the pyrimidine base of the terminal base-pair through its α face. This is a general trend for the three disaccharides studied, maltose, cellobiose, and lactose. In contrast, the nonreducing pyranose ring stacks on top of the base-paired purine, interacting through its β face for cellobiose and lactose but through its α face for maltose. In fact, the three disaccharides present well-defined conformations within the carbohydrate oligonucleotide conjugates that are quite similar to the ones observed for the free disaccharides.[25] This is confirmed by the interglycosidic angles obtained in the molecular dynamics calculations (Figure S4) and by the interglycosidic NOEs (Table S4). It is important to mention that the relative position of the disaccharides stacked on top of the terminal base pair in the different conjugates is very similar. Although no hydrogen bonds are observed between the carbohydrate and DNA, some hydrogen bonds are found between the two pyranose units [OH3(carb2) → O3(carb1) for conjugate **4** and OH3(carb2) → O5(carb1) for conjugates **5**, **6**, and **11**] and between the reducing pyranose ring and the phosphate group of the ethylene glycol linker [OH2(carb1) → PO_2^- (linker)].

When the structures obtained for cellobiose stacking on top of C−G or T−A base pairs (conjugates **5** and **11**, respectively) are compared (Figure 4), very few differences are observed no matter which base pair is located at the edge of the duplex. This suggests that the different stabilization induced by the carbohydrates on duplexes with terminal G−C or A−T base-pairs is not due to the intrinsic nature of carbohydrate−aromatic interaction, but on how carbohydrates affect the dynamic behavior of terminal base-pairs. NMR[26] and computational techniques[27] have shown that base-pair breathing movements are more intense in A−T than in G−C. NMR data indicate that carbohydrate interaction affects the dynamics of the terminal base-pairs, reducing their fraying. A possible explanation for these results may be that the enhanced entropic cost of reducing the fraying in more flexible terminal A−T base-pairs compensates the stabilization effect of carbohydrate capping. At the same time, it is important to note that the dipole moments of GC base pairs are much larger that those for AT base pairs.[28] If electrostatic interactions are an important factor in the interaction with the stacked carbohydrates, those differences could help to explain the stability found for GC pairs versus AT pairs.

Significance of the Carbohydrate−DNA Base Stacking Interactions. Our results suggest that stacking plays a significant role in naturally occurring carbohydrate−nucleic acid complexes. One of the most relevant examples of carbohydrate−RNA molecular recognition is the aminoglycoside binding to the 16S rRNA A-site.[29] Our findings suggest that the stacking of the 2′-amino-2′-deoxyglucose unit of different aminoglycosides on top of guanine 1491 makes an energetic contribution in aminoglycoside binding of the 16S rRNA A-site. Although electrostatic charge−charge interactions and hydrogen bonds between aminoglycosides and RNA are the most important features of the binding, carbohydrate−DNA base stacking present in all aminoglycosides−RNA structures[18,30] must also be energetically relevant. Nevertheless, Asensio et al.[31] have recently hypothesized that the stacking interactions observed in aminoglycosides binding to RNA where several amino groups are protonated might be reduced with respect to that usually observed for neutral oligosaccharides. According to the same authors, the stacking contribution to the overall binding will mainly depend on the extent of ammonium desolvation promoted by the hydrophobic aromatic rings in the complexed state.

Moreover, our finding that mono- and disaccharide−DNA base stacking interactions are energetically stabilizing has general implications in the design of new carbohydrate-based RNA binders, an important field due to the necessity of new and less toxic antibiotics.[32] Favorable stacking interactions can be used to modulate or combine with other better known carbohydrate−RNA molecular interactions, such as hydrogen bonding and electrostatic interactions. Similarly, the repetition of this saccharide−DNA base stacking binding-motif or its combination with other noncovalent molecular forces, such as aromatic−aromatic stacking interactions, may have potential applications in the

construction of new supramolecular structures or biobased nanomaterials.

CONCLUSIONS

We have shown that carbohydrate−DNA interactions are observed in a sugar-capped DNA double helix. Mono- and disaccharides, highly polar nonaromatic molecules, stack onto the terminal base pair of DNA duplexes as shown by a large number of NOE contacts. Moreover, these saccharides are capable of stabilizing DNA duplexes with terminal C−G or G−C base pairs. In contrast, no stabilization was observed when T−A or A−T was the terminal base pair quite possibly due to the entropic cost of interacting with a more dynamic edge of the DNA.

MATERIALS AND METHODS

Preparation of Carbohydrate Alcohols and Phosphoramidites. Synthesis of disaccharide alcohols **21**, **23**, and **25** and disaccharide phosphoramidites **17**−**19** was carried out by following the described methodology.[14] For the characterization of compounds **17**, **18**, **19**, **21**, **23**, and **25**, see the Supporting Information.

Synthesis of Carbohydrate−Oligonucleotide Conjugates 1−12. Carbohydrate−oligonucleotide conjugates were synthesized on an Applied Biosystems 394 synthesizer by using standard β-cyanoethylphosphoramidite chemistry. Oligonucleotide conjugates were synthesized either on low-volume 200 nmol (LV200) or 1.0 μmol scale and using the DMT-off procedure. Oligonucleotide supports were treated with 33% aqueous ammonia for 16 h at 55 °C, and then the ammonia solutions were evaporated to dryness and the conjugates were purified by reversed-phase HPLC in a Waters Alliance separation module with a PDA detector. HPLC conditions were as follows: Nucleosil 120 C18, 250 × 8 mm, 10 μm column; flow rate, 3 mL/min. A 27 min linear gradient 0−30% B (solvent A, 5% CH_3CN/95% 100 mM triethylammonium acetate (TEAA; pH 6.5); solvent B, 70% CH_3CN/30% 100 mM TEAA (pH 6.5)). For the characterization of conjugates **1**−**12**, see the Supporting Information.

Thermodynamic Measurements. Melting curves for the DNA conjugates were measured in a Perkin−Elmer Lambda 750 UV/vis spectrophotometer at 280 nm while the temperature was raised from 10 to 80 °C at a rate of 1.0 °C min^{-1}. Curve fits were excellent, with c^2 values of 10^6 or better, and the van't Hoff linear fits were quite good (r^2 = 0.98) for all oligonucleotides. Differences of less than 3% were observed between thermodynamic parameters as determined by $1/T_m$ versus ln[conjugate] plots and curve fittings. ΔG errors were calculated as described previously.[4a,20]

NMR Spectroscopy. Samples of all the conjugates and control duplexes were purified by HPLC, ion-exchanged with Dowex 50W resin and then suspended in 500 μL of either D_2O or H_2O/D_2O 9:1 in phosphate buffer, 100 mM NaCl, pH 7. NMR spectra were acquired in Bruker Avance spectrometers operating at 600 or 800 MHz and were processed with Topspin software. DQF-COSY, TOCSY, and NOESY experiments were recorded in D_2O. The NOESY spectra were acquired with mixing times of 150 and 300 ms, and the TOCSY spectra were recorded with standard MLEV-17 spin-lock sequence, and 80 ms mixing time. NOESY spectra in H_2O were acquired with 100 ms mixing time. In 2D experiments in H_2O, water suppression was achieved by including a WATERGATE[33] module in the pulse sequence prior to acquisition. Two-dimensional experiments in D_2O were carried out at temperatures ranging from 5 to 25 °C, whereas spectra in H_2O were recorded at 5 °C to reduce the exchange with water. The spectral analysis program Sparky[34] was used for semiautomatic assignment of the NOESY cross-peaks and quantitative evaluation of the NOE intensities. Distance constraints with their corresponding error bounds were incorporated into the AMBER potential energy by defining a flat-well potential term.

Structure Calculations. Structures were calculated with the SANDER module of the molecular dynamics package AMBER.[35] Starting models of the conjugate duplexes were built using the program SYBYL. The DNA moieties in the starting models were set to a standard B- canonical structure. These structures were taken as starting points for the AMBER refinement, which started with an annealing protocol in vacuo (using hexahydrated Na^+ counterions placed near the phosphates to neutralize the system). The resulting structures from in vacuo calculations were placed in the center of a water-box with around 4000 water molecules and 12 sodium counterions to obtain electroneutral systems. The structures were then refined including explicit solvent, periodic boundary conditions and the Particle-Mesh-Ewald method to evaluate long-range electrostatic interactions.[36] Force field parameters for the carbohydrate moieties were taken from GLYCAM.[37] The TIP3P model was used to describe water molecules.[38] The protocol for the constrained molecular dynamics refinement in solution consisted of an equilibration period of 160 ps using a standard equilibration process,[39] followed by four independent 500 ps runs. Averaged structures were obtained by averaging the last 20 ps of individual trajectories and further energy minimization of the structure. Analysis of the representative structures as well as the MD trajectories was carried out with the program MOLMOL[40] and the analysis tools of AMBER.

ASSOCIATED CONTENT

Supporting Information. Experimental procedures for the synthesis of compounds **17**−**19**, **21**, **23**, and **25** and their complete characterization. Characterization of carbohydrate oligonucleotide conjugates (COCs) **1**−**6**, **8**, **11**, and controls **13** and **15**. Examples of melting and van't Hoff curves of the COCs. NMR proton assignments, relevant NOEs, and chemical shift changes for conjugates **1**−**6**, **8**, **11**, and controls **13** and **15**. This material is available free of charge via the Internet at http://pubs.acs.org.

AUTHOR INFORMATION

Corresponding Author
jcmorales@iiq.csic.es

ACKNOWLEDGMENT

Financial support by Consejo Superior de Investigaciones Científicas (CSIC-PIF06-045), Ministerio de Ciencia e Innovación (grants CTQ2006-01123, CTQ2007-68014-C02-02, CTQ2009-13705, BFU2007-63287), Generalitat de Catalunya (2009/SGR/208), and Instituto de Salud Carlos III (CIBER-BNN, CB06_01_0019) is gratefully acknowledged. R.L. thanks CSIC for a JAE contract.

REFERENCES

(1) Rebek, J.; Askew, B.; Ballester, P.; Buhr, C.; Jones, S.; Nemeth, D.; Williams, K. *J. Am. Chem. Soc.* **1987**, *109*, 5033–5035.

(2) Newcomb, L. F.; Gellman, S. H. *J. Am. Chem. Soc.* **1994**, *116*, 4993–4994.

(3) Geoffrey, W. C.; Alex, R. D.; Lawrence, M. H.; Dennis, A. D.; Robert, H. G. *Angew. Chem., Int. Ed. Engl.* **1997**, *36*, 248–251.

(4) (a) Lokhov, S. G.; Pyshnyi, D. V. *FEBS Lett.* **1997**, *420*, 134–8. Petersheim, M.; Turner, D. H. *Biochemistry* **1983**, *22*, 256–63. (b) Senior, M.; Jones, R. A.; Breslauer, K. J. *Biochemistry* **1988**, *27*, 3879–85.

(5) (a) Guckian, K. M.; Schweitzer, B. A.; Ren, R. X. F.; Sheils, C. J.; Paris, P. L.; Tahmassebi, D. C.; Kool, E. T. *J. Am. Chem. Soc.* **1996**, *118*, 8182–8183. (b) Guckian, K. M.; Schweitzer, B. A.; Ren, R. X. F.; Sheils, C. J.; Tahmassebi, D. C.; Kool, E. T. *J. Am. Chem. Soc.* **2000**, *122*, 2213–2222. (c) Kim, T. W.; Kool, E. T. *J. Org. Chem.* **2005**, *70*, 2048–53. (d) Morales-Rojas, H.; Kool, E. T. *Org. Lett.* **2002**, *4*, 4377–80. (e) O'Neill, B. M.; Ratto, J. E.; Good, K. L.; Tahmassebi, D. C.; Helquist, S. A.; Morales, J. C.; Kool, E. T. *J. Org. Chem.* **2002**, *67*, 5869–75. (f) Morales, J. C.; Kool, E. T. *Biochemistry* **2000**, *39*, 12979–88. (g) Zhang, L.; Long, H.; Boldt, G. E.; Janda, K. D.; Schatz, G. C.; Lewis, F. D. *Org. Biomol. Chem.* **2006**, *4*, 314–22.

(6) (a) Kryatova, O. P.; Connors, W. H.; Bleczinski, C. F.; Mokhir, A. A.; Richert, C. *Org. Lett.* **2001**, *3*, 987–90. (b) Tuma, J.; Connors, W. H.; Stitelman, D. H.; Richert, C. *J. Am. Chem. Soc.* **2002**, *124*, 4236–46.

(7) Dogan, Z.; Paulini, R.; Rojas Stutz, J. A.; Narayanan, S.; Richert, C. *J. Am. Chem. Soc.* **2004**, *126*, 4762–3.

(8) Printz, M.; Richert, C. *J. Comb. Chem.* **2007**, *9*, 306–20.

(9) (a) Balaz, M.; Holmes, A. E.; Benedetti, M.; Proni, G.; Berova, N. *Bioorg. Med. Chem.* **2005**, *13*, 2413–21. (b) Balaz, M.; Holmes, A. E.; Benedetti, M.; Rodriguez, P. C.; Berova, N.; Nakanishi, K.; Proni, G. *J. Am. Chem. Soc.* **2005**, *127*, 4172–3.

(10) Matray, T. J.; Kool, E. T. *J. Am. Chem. Soc.* **1998**, *120*, 6191–6192.

(11) Zahn, A.; Leumann, C. J. *Chem.-Eur. J.* **2008**, *14*, 1087–1094.

(12) Kaufmann, M.; Gisler, M.; Leumann, C. J. *Angew. Chem., Int. Ed.* **2009**, *48*, 3810–3.

(13) Bleczinski, C. F.; Richert, C. *J. Am. Chem. Soc.* **1999**, *121*, 10889–10894.

(14) Morales, J. C.; Reina, J. J.; Díaz, I.; Aviñó, A.; Nieto, P. M.; Eritja, R. *Chem.-Eur. J.* **2008**, *14*, 7828–7835.

(15) Moore, M. H.; Hunter, W. N.; d'Estaintot, B. L.; Kennard, O. *J. Mol. Biol.* **1989**, *206*, 693–705.

(16) Ikemoto, N.; Kumar, R. A.; Ling, T. T.; Ellestad, G. A.; Danishefsky, S. J.; Patel, D. J. *Proc. Natl. Acad. Sci. U.S.A.* **1995**, *92*, 10506–10.

(17) Hansen, M.; Hurley, L. *J. Am. Chem. Soc.* **1995**, *117*, 2421–2429.

(18) Vicens, Q.; Westhof, E. *Biopolymers* **2003**, *70*, 42–57.

(19) Dogan, Z.; Paulini, R.; Rojas Stutz, J. A.; Narayanan, S.; Richert, C. *J. Am. Chem. Soc.* **2004**, *126*, 4762–3.

(20) Ohmichi, T.; Nakano, S.; Miyoshi, D.; Sugimoto, N. *J. Am. Chem. Soc.* **2002**, *124*, 10367–72.

(21) Bommarito, S.; Peyret, N.; SantaLucia, J., Jr. *Nucleic Acids Res.* **2000**, *28*, 1929–34.

(22) (a) Ho, W. C.; Steinbeck, C.; Richert, C. *Biochemistry* **1999**, *38*, 12597–606. (b) Gomez-Pinto, I.; Marchan, V.; Gago, F.; Grandas, A.; Gonzalez, C. *ChemBioChem* **2003**, *4*, 40–9.

(23) (a) Tuma, J.; Paulini, R.; Rojas Stutz, J. A.; Richert, C. *Biochemistry* **2004**, *43*, 15680–7. (b) Tuma, J.; Richert, C. *Biochemistry* **2003**, *42*, 8957–65.

(24) (a) Boraston, A. B.; Bolam, D. N.; Gilbert, H. J.; Davies, G. J. *Biochem. J.* **2004**, *382*, 769–781. (b) Kogelberg, H.; Solis, D.; Jimenez-Barbero, J. *Curr. Opin. Struct. Biol.* **2003**, *13*, 646–53.

(25) Cheetham, N. W.; Dasgupta, P.; Ball, G. E. *Carbohydr. Res.* **2003**, *338*, 955–62.

(26) Kearns, D. R. *CRC Crit. Rev. Biochem.* **1984**, *15*, 237–90.

(27) Krueger, A.; Protozanova, E.; Frank-Kamenetskii, M. D. *Biophys. J.* **2006**, *90*, 3091–3099.

(28) Parthasarathi, R.; Subramanian, V. *Chem. Phys. Lett.* **2006**, *418*, 530–534.

(29) Pilch, D. S.; Kaul, M.; Barbieri, C. M.; Kerrigan, J. E. *Biopolymers* **2003**, *70*, 58–79.

(30) Walter, F.; Vicens, Q.; Westhof, E. *Curr. Opin. Chem. Biol.* **1999**, *3*, 694–704.

(31) Vacas, T.; Corzana, F.; Jimenez-Oses, G.; Gonzalez, C.; Gomez, A. M.; Bastida, A.; Revuelta, J.; Asensio, J. L. *J. Am. Chem. Soc.* **2010**, *132*, 12074–90.

(32) Hermann, T. *Curr. Opin. Struct. Biol.* **2005**, *15*, 355–66. Hermann, T. *Cell. Mol. Life Sci.* **2007**, *64*, 1841–52.

(33) Piotto, M.; Saudek, V.; Sklenar, V. *J. Biomol. NMR* **1992**, *2*, 661–5.

(34) Goddard, D. T.; Kneller, G. *Sparky*, 3rd ed.; University of California: San Francisco, CA, 2004.

(35) Case, D. A.; Pearlman, D. A.; Caldwell, J. W.; T., E. C., III; Ross, W. S.; Simmerling, C. L.; Darden, T. A.; Merz, K. M.; Stanton, R. V.; Cheng, A. L.; Vincent, J. J.; Crowley, M.; Ferguson, D. M.; Radmer, R. J.; Seibel, G. L.; Singh, U. C.; Weiner, P. K.; Kollman, P. A. *AMBER*, 5th ed.; University of California: San Francisco, CA, 1997.

(36) Darden, T. E.; York, D.; Pedersen, L. *J. Chem. Phys.* **1993**, *98*, 10089–10092.

(37) Woods, R. J.; Dwek, R. A.; Edge, C. J.; Fraser-Reid, D. *J. Phys. Chem.* **1995**, *99*, 3832–3839.

(38) Jorgensen, W. L.; Chandrasekhar, J.; Madura, J. D.; Impey, R. W.; Klein, M. L. *J. Chem. Phys.* **1983**, *79*, 926–935.

(39) Soliva, R.; Monaco, V.; Gomez-Pinto, I.; Meeuwenoord, N. J.; Marel, G. A.; Boom, J. H.; Gonzalez, C.; Orozco, M. *Nucleic Acids Res.* **2001**, *29*, 2973–85.

(40) Koradi, R.; Billeter, M.; Wuthrich, K. *J. Mol. Graphics* **1996**, *14*, 29–32.

(41) Ghose, A. K.; Crippen, G. M. *J. Chem. Inf. Comput. Sci.* **1987**, *27*, 21–35.